ChemPubSoc Europe

DOI: 10.1002/cssc.201403230

CHEMSUSCHEM Full Papers

Polar Group and Defect Engineering in a Metal–Organic Framework: Synergistic Promotion of Carbon Dioxide Sorption and Conversion

Zhuo-Rui Jiang,[a] Hengwei Wang,[a] Yingli Hu,[a] Junling Lu,[a] and Hai-Long Jiang*[a, b]

A sulfone-functionalized metal–organic framework (MOF), USTC-253, has been synthesized that exhibits a much higher CO_2 uptake capacity (168–182%) than the corresponding unfurnished MOFs. The introduction of trifluoroacetic acid (TFA) during the synthesis of USTC-253 affords defect-containing USTC-253-TFA with exposed metal centers, which has an increased CO_2 uptake (167%) compared to pristine USTC-253. USTC-253-TFA exhibits a very high ideal adsorption solution theory selectivity ($S = 75$) to CO_2 over N_2 at 298 K. In addition, USTC-253-TFA demonstrates good catalytic activity and recyclability in the cycloaddition of CO_2 and epoxide at room temperature under 1 bar CO_2 pressure as a result of the presence of Lewis and Brønsted acid sites, which were evaluated by diffuse reflectance infrared Fourier transform spectroscopy with a CO probe molecule. We propose that the CO_2 adsorption capability has a positive correlation with the catalytic performance toward CO_2 conversion.

Introduction

With the rising standards of living and the growing population worldwide, the demand on the combustion of fossil fuels (coal, petroleum, and natural gas) is increasing, which is believed to be the main contribution to the increasing anthropogenic CO_2 emissions and the worsening worldwide climatic situation. There is an urgent need for strategies to depress global atmospheric concentrations of greenhouse gases (mainly CO_2). Carbon capture and sequestration (CCS) has been proposed as an effective approach to meet this challenge, which comprises the capture of CO_2 from power plants, followed by compression, transportation, and permanent storage. Of these processes, the removal of CO_2 from flue gas at power plants is the most energy- and cost-intensive, as the state-of-the-art technology for the widely accepted amine-based wet-scrubbing approach still suffers from a high regeneration cost, equipment corrosion, and solvent boil off.[1] It is imperative, although challenging, to develop functional materials that feature high CO_2 selectivity over other components in flue gas with a low-energy penalty during regeneration. In this context, porous sorbents that adsorb CO_2 preferentially over N_2 based on a physisorption mechanism with low energy requirements could be an alternative and promising choice.

However, in addition to the storage of CO_2 underground as a waste with a cost of disposal, the development of methods to activate and convert CO_2 catalytically to fuels or/and high-value chemicals is an attractive research goal. Although CO_2 has inherent thermodynamic stability and inert nature as a C1 feedstock, it has been demonstrated that CO_2 can be converted into many useful chemicals, which are used increasingly in industrial process.[2,3] Particularly, the coupling of CO_2 with epoxides into cyclic carbonates, which are useful chemical intermediates in the production of plastics, organic solvents, and others, is a very efficient route for CO_2 utilization.[3] A considerable number of homogeneous catalysts, which includes ionic liquids, alkali metal salts, Schiff bases, and metal-centered salen or porphyrin complexes, were reported to be effective for the conversion,[4] although these systems have inherent limitations in terms of the separation of the product and catalyst recycling. To address this issue, various heterogeneous catalysts have been investigated for the coupling of CO_2 with epoxides.[5] However, most of these solids exert their activity at relatively high temperatures and some require the presence of cosolvents, although they have overcome the previous difficulty of catalyst recovery. It is desirable to develop a highly efficient and recyclable catalyst for the conversion of CO_2 under mild conditions.

To meet the dual challenge of CO_2 capture and conversion, a relatively new class of crystalline porous materials, metal–organic frameworks (MOFs),[6] could be ideal candidates. MOFs have captured widespread interest because of their designable and tunable structures and wide applications in various fields, especially for CO_2 capture and heterogeneous catalysis.[7–11]

[a] Z.-R. Jiang, H. Wang, Y. Hu, Prof. Dr. J. Lu, Prof. Dr. H.-L. Jiang
Hefei National Laboratory for Physical Sciences at the Microscale
CAS Key Laboratory of Soft Matter Chemistry
Collaborative Innovation Center of Suzhou Nano Science and Technology
School of Chemistry and Materials Science
University of Science and Technology of China
Hefei, Anhui 230026 (P.R. China)
E-mail: jianglab@ustc.edu.cn

[b] Prof. Dr. H.-L. Jiang
State Key Laboratory of Structural Chemistry
Fujian Institute of Research on the Structure of Matter
Chinese Academy of Sciences
Fuzhou, Fujian 350002 (P.R. China)

Supporting Information for this article is available on the WWW under http://dx.doi.org/10.1002/cssc.201403230.

MOFs offer a promising platform for CO_2 capture because they have very high surface areas and gas sorption capacity as well as a tailorable pore surface/environment that can facilitate selective CO_2 binding.[10] In addition to the crucial role of coordinatively unsaturated metal sites (CUSs) for CO_2 adsorption, given the polarizability and quadrupole moment of the acidic oxide CO_2 molecule, the polarizing and alkaline functional groups involved in MOFs lead to enhanced CO_2 capture.[12] Most recently, trifluoroacetic acid (TFA)/acetic acid and HCl have been found to cause the structural defects in MOFs if they are involved in the modulated synthesis. The defect sites are able to enhance the CO_2 adsorption and catalytic properties significantly.[13] In addition, most MOFs contain CUSs as Lewis acid sites, bridging –OH groups with Brønsted acidity, and other catalytically active sites on the organic linkers, which make MOFs applicable for heterogeneous catalysis.[11] The high-density active sites distributed uniformly throughout the framework are easily accessible, and the pore structure facilitates the transfer of substrates and products. Therefore, MOFs with Lewis/Brønsted acid sites as well as basic sites may offer excellent activity for CO_2 conversion and utilization by cycloaddition with epoxides. To date, several MOFs with Lewis acid sites have been reported for the catalytic cycloaddition of CO_2 with epoxides, most of which require high-pressure and/or high-temperature conditions.[14] Only two Cu-MOFs, typically with mild stability, have been developed recently to accomplish such a conversion with 1 bar CO_2 at room temperature.[15] It is agreed that stability is of prime importance for practical implementation in heterogeneous catalysis. Moreover, to the best of our knowledge, the correlation between the CO_2 sorption performance and conversion by MOFs has not been explored yet.

With the aforementioned considerations, a stable Al-based MOF, denoted as USTC-253 (USTC = University of Science and Technology of China), has been synthesized by the reaction of $Al(NO_3)_3{\cdot}9H_2O$ and 4,4′-dibenzoic acid-2,2′-sulfone (Sbpdc) in DMF. For comparison, Sbpdc was replaced with 4,4′-biphenyldicarboxylic acid (bpdc) and 2,2′-bipyridine-5,5′-dicarboxylate acid (bpydc) under the same conditions to afford elongated MIL-53 (EL-MIL-53)[16a] and MOF-253,[16b] respectively, which have the same structural topology but substituted organic linkers. Remarkably, the introduction of TFA into USTC-253 leads to USTC-253-TFA, which has almost the same structure as USTC-253 with a certain amount of structural defects. The resulting USTC-253 with polar sulfone groups exhibits a significantly higher CO_2 adsorption than of EL-MIL-53 and MOF-253. The presence of defects leads to the generation of CUSs and Lewis acid sites, which further enhances the CO_2 capture capability. More importantly, USTC-253-TFA with both Brønsted and Lewis acid sites possesses a high activity and satisfactory recyclability toward catalytic CO_2 cycloaddition under ambient conditions. As far as we know, this work is the first report of the synergistic improvement of CO_2 uptake by the co-involvement of polar functional groups and structural defects in the MOF. In addition, for the first time, the correlation between CO_2 sorption performance and catalytic conversion has been proposed.

Results and Discussion

Crystal structure and general characterization

Solvothermal reactions of $Al(NO_3)_3{\cdot}9H_2O$ and organic linker (Sbpdc, bpdc, or bpydc) in DMF at 393 K yielded a white polycrystalline powder of Al(OH)(L) (L = Sbpdc, USTC-253; bpdc, EL-MIL-53; bpydc, MOF-253). Powder X-ray diffraction (PXRD) studies demonstrated their identical structural topology and good crystallinity (Figure S3). Notably, the deviation from linearity (~160°) in Sbpdc does not affect the coordination modes of the ligand, and this linker is able to form an isoreticular structure with MOF-253 and EL-MIL-53. In the structure, Al^{III} is coordinated octahedrally by four carboxylate O atoms in the plane and two O atoms from hydroxyl groups located at the axial positions. The Al–OH chains, formed by the alternate array of Al^{III} and hydroxyl groups, are bridged by the organic linkers to give a 3D network with rectangular channels of around 1.1×1.1 nm^2 (Figure 1).

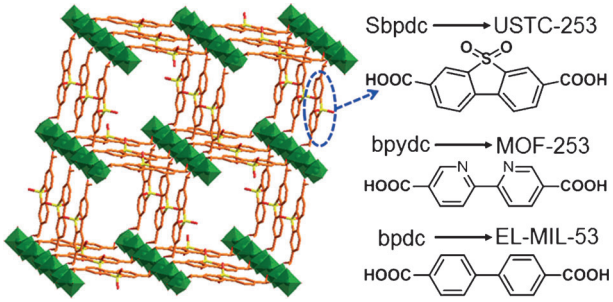

Figure 1. Structure of USTC-253 (left) and the ligands involved in the structures of USTC-253, MOF-253, and El-MIL-53 (right).

It is well known that single crystals of Al-MOFs are extremely difficult to obtain because the coordination between Al^{III} and carboxylate ligands is rapid and the inert coordination bonds between Al^{III} cations and carboxylate anions make ligand-exchange reactions slow, which is unfavorable for crystal growth. A large amount of a small monocarboxylic acid, such as TFA, which behaves as a modulator, is proposed to first coordinate to the Al^{III} centers, which is followed by a relatively slow ligand exchange between the acid and Sbpdc. As expected, with such a modulated synthetic strategy, the TFA involved in the synthesis endows the obtained USTC-253-TFA with a remarkably improved crystallinity (Figures S3 and S4), which would be beneficial for subsequent functional applications.[12b,17] SEM images indicate that the USTC-253-TFA particles are rod shaped, of approximately 300 nm in size, and aggregate to larger particles in the microscale, whereas USTC-253 nanoflakes of approximately 200 nm in diameter have very few aggregations (Figure S5). In addition, similar to the synthesis of UiO-66,[13a,b] given the unavoidable incomplete ligand exchange, the participation of TFA as a modulator in the reaction will lead to the formation of vacancies and missing-linker defects

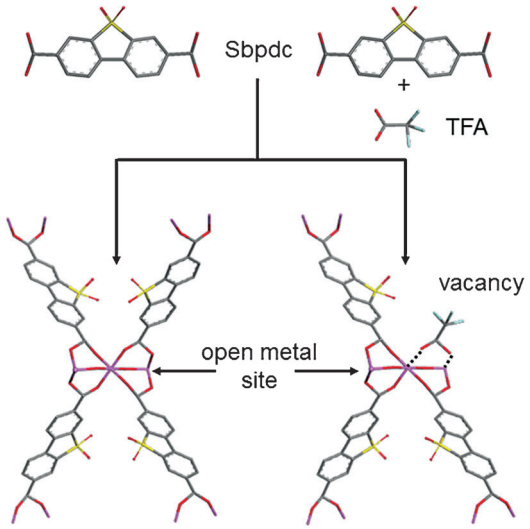

Figure 2. Synthesis of USTC-253 (left) and defect-engineered USTC-253-TFA (right).

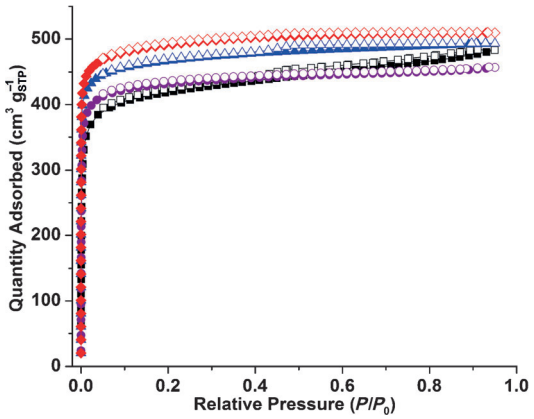

Figure 3. N_2 sorption isotherms of USTC-253 (blue), USTC-253-TFA (red), EL-MIL-53 (black), and MOF-253 (purple) at 77 K. Solid and open circles represent adsorption and desorption data, respectively.

in the structure (Figure 2), which will bring new coordinately unsaturated metal centers that act as the desired Lewis acid sites for the enhanced CO_2 capture and catalytic conversion of USTC-253-TFA. Elemental analysis shows that the S content in USTC-253 and USTC-253-TFA is 8.31 and 8.13%, respectively, which is close to the theoretical value of 9.25%. The slightly lower experimental values could be ascribed to the unavoidable water adsorbed in the samples before measurement. The introduction of TFA during USTC-253 synthesis leads to a slightly lower S content, which is in agreement with the presence of missing linkers in the structure of USTC-253-TFA. The IR spectrum of USTC-253 shows peaks at $\tilde{\nu}=1307$ and 1133 cm^{-1}, which correspond to the symmetric and asymmetric stretches of the $-SO_2$ group, respectively (Figure S6).[18] Thermogravimetric (TG) analysis of as-synthesized USTC-253 demonstrates that it has a similar thermostability up to 450 °C in N_2 to EL-MIL-53 and MOF-253 (Figure S7). The weight loss between 450 and 700 °C corresponds to the combustion of the organic part. In the TG profile of USTC-253-TFA, the loss of TFA is discerned as a clear step between 190 and 300 °C.

To examine the pore characteristics, N_2 sorption for all these MOFs was measured and exhibits type I isotherms at 77 K (Figure 3), which indicates the typical character of microporous materials. The BET surface areas are fitted to be 1800, 1892, 1599, and 1671 m^2 g^{-1}, respectively, for USTC-253, USTC-253-TFA, EL-MIL-53, and MOF-253, with corresponding pore volumes of 0.76, 0.79, 0.74, and 0.71 cm^3 g^{-1}. USTC-253-TFA has the highest surface area and pore volume of these materials, although its additional pore space is occupied by $-SO_2$ groups, which is mainly attributed to the presence of missing linkers and the improved crystallinity of USTC-253-TFA. This result agrees well with a previous report.[13a] The considerable surface area, high free volume, nanosized free channels, accessible exposed metal sites, and good stability for the MOF could endow it with a very high potential in CO_2 capture, heterogeneous catalysis, and other functional applications.

Brønsted and Lewis acidity characterization

To evaluate the presence of Brønsted and Lewis acidic sites on USTC-253-TFA, diffuse reflectance infrared Fourier transform (DRIFT) spectroscopy of CO adsorption was performed at 150 K by using a Nicolet iS10 spectrometer with a mercury cadmium telluride (MCT) detector and a low-temperature reaction chamber (Praying Mantis Harrick). The background was measured for the activated USTC-253-TFA. Upon CO adsorption, two peaks at $\tilde{\nu}=2147$ and 2137 cm^{-1} with a shoulder at $\tilde{\nu}=$ 2130 cm^{-1} were observed along with the broad gaseous CO peak (Figure 4a and b) in the ν(CO) vibrational region. Meanwhile, two negative peaks at $\tilde{\nu}=3714$ and 3693 cm^{-1} appeared, which became more intense as the CO dosage increased. Next, we stopped the CO dosage and continued to collect DRIFT spectra as the sample temperature increased

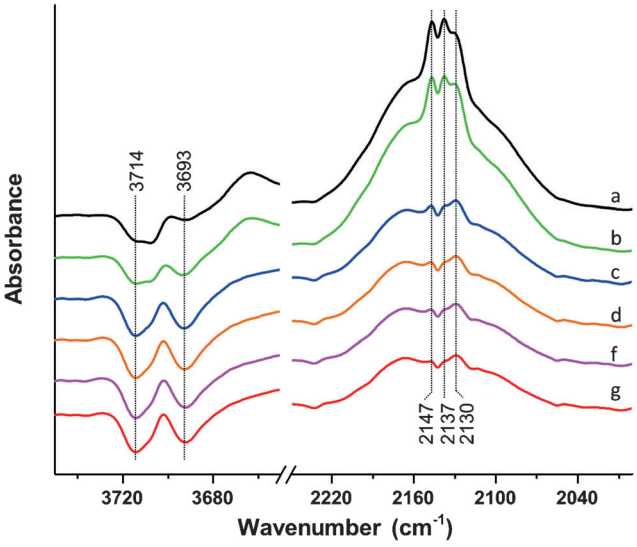

Figure 4. a, b) DRIFT spectra of CO adsorption on USTC-253-TFA at 150 K with increasing CO coverage and c–g) spectra collected at decreasing CO coverage and increasing temperatures.

slowly and the CO coverage decreased (Figure 4c–g). We observed that the intensity of the peak at $\tilde{\nu}=2130\ cm^{-1}$ decreased more slowly than that of the peaks at $\tilde{\nu}=2147$ and 2137 cm^{-1}. Therefore, the latter two peaks are assumed to correspond to physisorbed CO, and the former is likely to be the result of chemisorbed CO at Lewis acidic sites.[19a] In contrast, the intensity of the two negative peaks at $\tilde{\nu}=3714$ and 3693 cm^{-1} was almost constant during this process. These two negative peaks can be attributed to the disturbance of the ν(OH) vibration of the sample because of the formation a hydrogen bond with the CO molecule, a C-adduct, which indicates the existence of Brønsted acidic sites on USTC-253-TFA.[19b] In summary, the DRIFT spectra of CO adsorption shown in Figure 4 demonstrate the presence of both Brønsted and Lewis acidity, which is supported by subsequent catalytic experiments.

CO_2 sorption

Low-pressure CO_2 sorption was measured for USTC-253, EL-MIL-53, and MOF-253 at 273 and 298 K, respectively. MOF-253 presents a slightly higher CO_2 sorption capability than EL-MIL-53 at both 273 and 298 K because of the bipyridine N atoms involved in the framework of the former (Figure 5a). In contrast, the CO_2 sorption of USTC-253 at 1 bar is much higher and reaches 82.4 and 47.8 $cm^3\,g^{-1}$ at 273 and 298 K, respectively, which represents a 182% increase compared to that of EL-MIL-53 at 273 K (174% at 298 K) and a 168% increase compared that of to MOF-253 at 273 K (171% at 298 K). The enhanced CO_2 adsorption in USTC-253 could be attributed to the presence of polar sulfone groups, which enable strong interactions with CO_2 molecules. From this analysis, it is understandable that the heat of adsorption (Q_{st}) of USTC-253, which has sulfone groups, is higher than that of MOF-253, which bears N donor groups, whereas EL-MIL-253 has the lowest heat of adsorption for CO_2 (Figure 5b).

In addition to the effect of the polar sulfone group, structural defects are also beneficial to CO_2 adsorption.[13] As mentioned above, to generate structural defects by eliminating a few organic linkers, TFA as a modulator was introduced into the synthetic system for USTC-253. The unsaturated metal sites in the MOF created by structural defects would increase its interaction with CO_2 molecules and thus improve its CO_2 uptake capacity.[13d] A suitable amount of TFA is important to achieve the optimized result as the modulation ability is weak with a small amount of TFA and the MOF would not crystallize and form with too much TFA. As a result, the optimized USTC-253-TFA, obtained with TFA at 12.8 times the molar amount of Sbpdc, adsorbs 137.5 and 64.6 $cm^3\,g^{-1}$ CO_2 at 1 bar and 273 and 298 K (Figure 6a), respectively, with a heat of adsorption of 25.5 $kJ\,mol^{-1}$.

Both the CO_2 sorption capability and the zero-coverage isosteric heat of adsorption for USTC-253-TFA are significantly higher than those of USTC-253, which does not have defects (Figure 6b). The improvement could be explained because exposed metal centers promote the CO_2 sorption as the remaining TFA is volatile and labile and would be removed readily during the MOF activation process to offer not only coordinatively unsaturated metal sites but also more free space in the MOF pores, which could reasonably enable a higher CO_2 sorption. As far as we know, this is the first work that reports MOFs with polar functional groups and structural defects that could improve the CO_2 uptake capability synergistically.

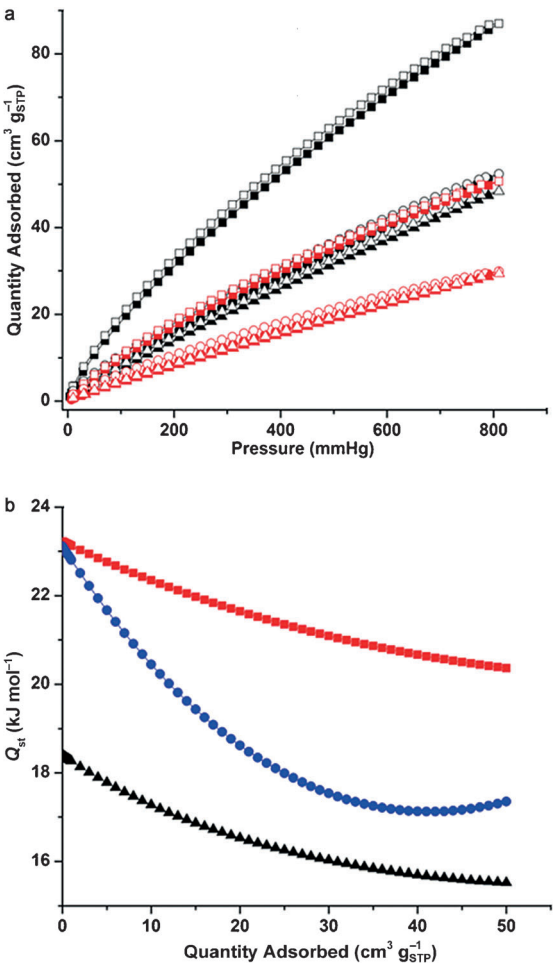

Figure 5. a) CO_2 adsorption (solid symbols) and desorption (open symbols) curves for USTC-253 (squares), MOF-253 (circles), and EL-MIL-53 (triangles) at 273 (black) and 298 K (red). b) Heat of adsorption for USTC-253 (■), MOF-253 (●), and EL-MIL-53 (▲).

USTC-253-TFA not only possesses the best CO_2 sorption capability among all of the other MOFs in this work but also exhibits excellent reproducibility with exactly the same adsorption amount during five cycles of CO_2 sorption (Figure S8), which is mainly attributed to its stable nature. Stability studies have indicated that the framework of USTC-253-TFA remains after storage in a humid environment for over 28 h, which is demonstrated by the retained PXRD profile (Figure S9). Moreover, with a significant CO_2 sorption capability, USTC-253-TFA hardly adsorbs N_2 under the same conditions (Figure S10), which demonstrates its desirable selective CO_2 sorption over N_2 ($S=75$) under postcombustion conditions (generally, 15% CO_2 and 85% N_2) at 298 K and 1 bar according to the ideal adsorption solution theory (IAST; Figure S11).[20]

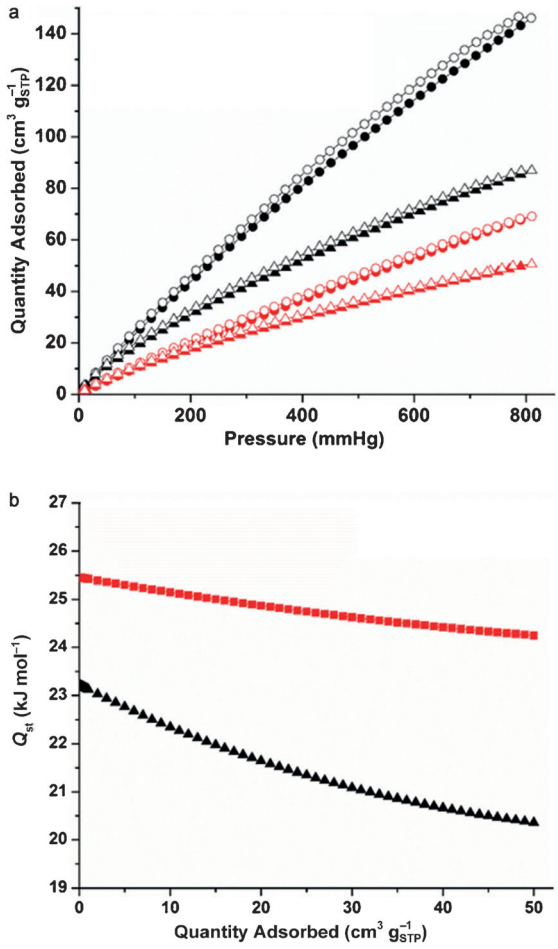

Figure 6. a) CO_2 adsorption (solid symbols) and desorption (open symbols) for USTC-253 (triangles) and USTC-253-TFA (circles) measured at 273 (black) and 298 K (red). b) Heat of adsorption of USTC-253 (▲) and USTC-253-TFA (■).

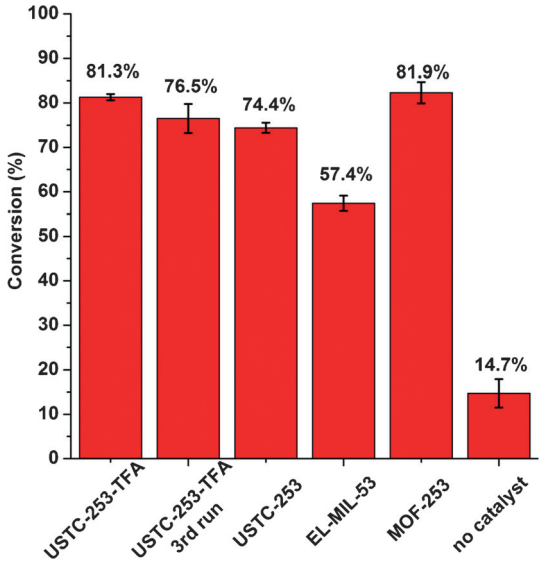

Figure 7. Catalytic conversion of CO_2 cycloaddition with propylene oxide over different catalysts. Reaction conditions: propylene oxide (28.6 mmol), catalyst (0.289 mmol), TBAB (1.86 mmol), CO_2 pressure (1 bar), 25 °C, 72 h. The error bars represent the standard deviations of the activities.

Cycloaddition of CO_2 and propylene oxide under mild conditions

In addition to the CO_2 capture capability, CO_2 cycloaddition with propylene oxide as a model substrate has been investigated for the utilization of CO_2 to useful high-value chemicals. A few MOFs with Lewis acid sites serve as heterogeneous catalysts for the cycloaddition of CO_2 and epoxides, although most of these reactions require high pressure (>3 MPa) and temperature (>100 °C) to turn greenhouse gases into environmentally friendly industrial materials. The harsh reaction conditions require a high energy cost and restrict the practical application of this type of reaction. Given the high CO_2 adsorption capability at room temperature and the presence of high-density and easily accessible Brønsted and Lewis acid active sites in USTC-253-TFA, this material could be a promising catalyst for CO_2 cycloaddition at room temperature and 1 bar pressure. USTC-253-TFA demonstrates highly efficient catalytic activity for the cycloaddition of propylene oxide with CO_2 into propylene carbonate in the presence of nBu$_4$NBr (TBAB) as a cocatalyst at room temperature and 1 bar CO_2 pressure with a yield of 81.3% in 72 h (Figure 7). The catalytic performance is better than that of homogeneous $Al(NO_3)_3$ (72.3% yield) and Sbpdc (29.5% yield) under the same conditions. Control experiments were conducted for USTC-253, EL-MIL-53, and MOF-253. USTC-253-TFA outperforms defect-free USTC-253, which exhibits a propylene carbonate yield of 74.4% in 72 h under similar conditions (Figure 7). The activity difference is mainly ascribed to the defect-induced coordinatively unsaturated metal centers in USTC-253-TFA that behave as Lewis acid sites and allow the conversion. In comparison, EL-MIL-53 has a moderate activity toward propylene carbonate with a yield of 57.4% in 72 h. USTC-253 and EL-MIL-53 have similar structures and the same amount of Brønsted acidic sites, and it is generally accepted that the additional $-SO_2$ group in USTC-253 does not affect the catalytic process. Therefore, we reasoned that the much higher catalytic activity of USTC-253 for CO_2 cycloaddition under ambient conditions should be mainly attributed to the higher CO_2 adsorption capability, which would promote the interactions between substrates and active sites greatly and thus improve the CO_2 conversion. To the best of our knowledge, this is the first attempt to establish the relationship between CO_2 adsorption and CO_2 cycloaddition activity for MOFs. MOF-253 reveals a very good catalytic conversion for CO_2 cycloaddition with a yield of 81.9% under similar conditions, although its CO_2 adsorption is not significantly high compared with that of USTC-253. The Brønsted acid sites and basic bipyridine N sites in the structure are responsible for its high catalytic activity.[14d]

In view of the results mentioned above, the introduction of a certain amount of TFA during USTC-253 synthesis will greatly enhance the CO_2 capture ability and generate Lewis acidic exposed metal sites, which, together with the existed Brønsted acidity, account for the excellent catalytic performance of USTC-253-TFA. Significantly, the catalyst is recycled readily by simple filtration and maintains its catalytic activity over three

cycles thanks to its good stability (Figure 7). The PXRD pattern of USTC-253-TFA demonstrates its intact framework after the reaction (Figure S12).

Some classical MOFs, for example, MIL-101, UiO-66, ZIF-8, and MIL-53,[21] which have commendable stability, have been studied widely for gas sorption and catalysis applications. For comparison, these MOFs have also been employed as catalysts for CO_2 cycloaddition reaction with propylene oxide. USTC-253-TFA has the highest catalytic activity among all these catalysts under the same conditions (Figure 8a), although MIL-101 and defect-containing UiO-66 comprise Lewis acid sites, and MIL-53 has a similar structure and smaller pore sizes than USTC-253-TFA. ZIF-8 shows the worst activity because of the lack of Lewis acid or base sites in the structure. In addition, CO_2 cycloaddition with epoxides substituted with different functional groups has been examined over USTC-253-TFA, and all epoxides exhibited modest conversions (Figure 8b).

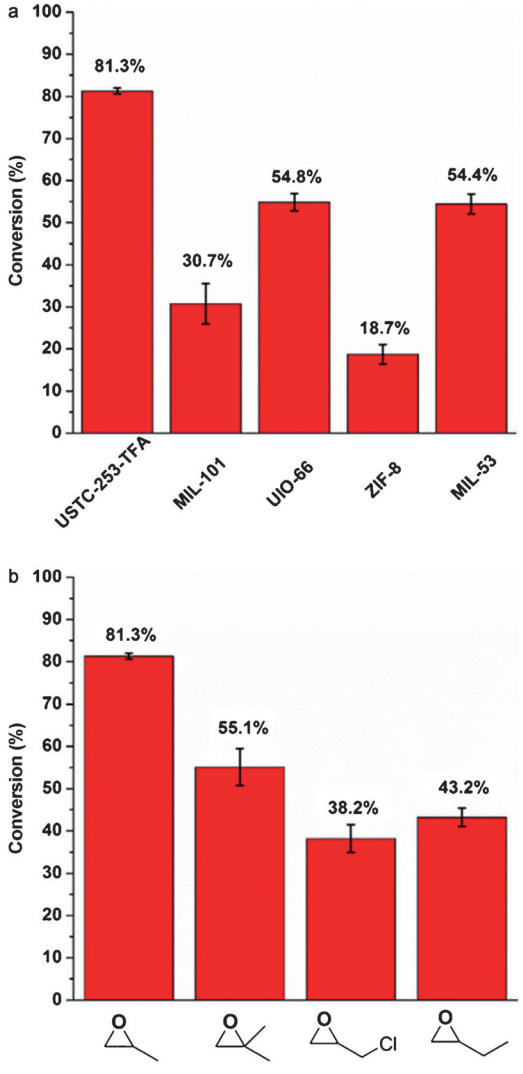

Figure 8. Catalytic conversion of CO_2 cycloaddition a) with propylene oxide over USTC-253-TFA and diverse classical MOFs and b) with epoxides substituted with different functional groups over USTC-253-TFA. Reaction conditions: epoxide (28.6 mmol), catalyst (0.289 mmol), TBAB (1.86 mmol), CO_2 pressure (1 bar), 25 °C, 72 h. The error bars represent the standard deviations of the activities.

These experimental results are of great importance to process anthropogenic CO_2 emission. Upon exposure to a CO_2 environment, USTC-253-TFA would adsorb CO_2 and gradually transform this raw material to propylene carbonate during the continuous introduction of epoxide into the reaction system. Based on some previous reports, a tentative mechanism is proposed for the cycloaddition of CO_2 and epoxide into cyclic carbonate over USTC-253-TFA (Figure 9). First, the epoxide binds to the Brønsted or Lewis acid sites in USTC-253-TFA through the O atom of the epoxide, which leads to the activation of the epoxy ring. Subsequently, the less-hindered C atom of the coordinated epoxide is attacked by Br^-, which is generated from TBAB, to open the epoxy ring. An alkylcarbonate anion is formed followed by the interaction of CO_2 with the oxygen anion of the opened epoxy ring. Through the final ring-closing step, the alkylcarbonate anion is converted into the cyclic carbonate, and simultaneously, TBAB is recycled. High-density and easily accessible Brønsted and Lewis acid sites could enhance the synergistic effect with TBAB to promote the CO_2 cycloaddition reaction. Consequently, USTC-253-TFA possesses a high catalytic activity for the conversion of CO_2 into cyclic carbonates under ambient conditions.

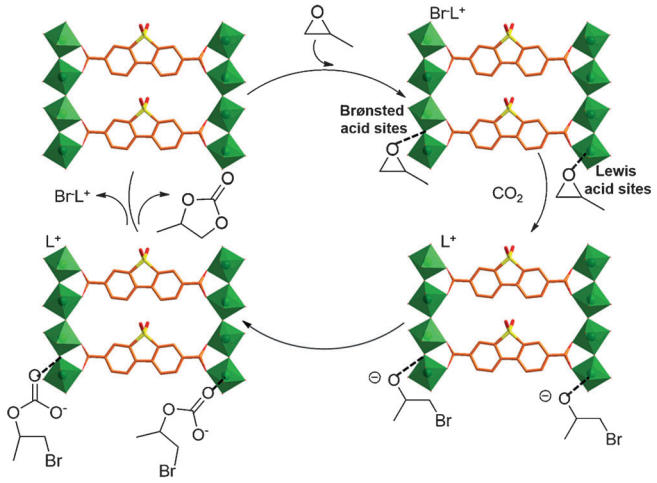

Figure 9. Proposed catalytic mechanism for the CO_2 cycloaddition of epoxide into cyclic carbonate over USTC-253-TFA.

The presence of both Lewis base and acid sites is desired to allow the reaction to proceed.[4d, 14d] The Lewis base sites could partly replace TBAB to activate CO_2 molecules, which subsequently attacks epoxide adsorbed on the Lewis acid sites, and thus facilitates the reaction. Such a mechanism accounts for the high catalytic activity of MOF-253, which bears both Brønsted acid and Lewis base sites.

Conclusions

A stable, Al-based metal–organic framework (MOF), USTC-253, isoreticular to MOF-253, was constructed by replacing bipyri-

dine-5,5′-dicarboxylate acid ligands with sulfone-functionalized 4,4′-dibenzoic acid-2,2′-sulfone. The introduction of a certain amount of trifluoroacetic acid (TFA) as the modulator during the synthesis of USTC-253 affords USTC-253-TFA, in which the structural defects led to the generation of exposed metal centers as Lewis acid sites upon activation. Given the presence of polar sulfone groups and exposed metal sites, USTC-253-TFA has as superior CO_2 adsorption capability to defect-free USTC-253, isoreticular MOF-253, and MIL-53. This is the first report on the synergistic enhancement of CO_2 sorption by the co-incorporation of polar functional groups and structural defects in MOFs. In addition, USTC-253-TFA exhibits a satisfactory catalytic activity and recyclability for CO_2 utilization by cycloaddition with epoxides to cyclic carbonates at room temperature and 1 bar CO_2 pressure that surpasses that of parent USTC-253 and some classical MOFs. The presence of high-density and easily accessible Brønsted and Lewis acid sites, which is demonstrated by diffuse reflectance infrared Fourier transform spectroscopy of CO adsorption, accounts for the superiority of USTC-253-TFA, and a catalytic mechanism has been proposed. TFA in the synthesis replaces part of the organic linkers to create extra Lewis acid sites, which are beneficial to not only CO_2 uptake but also to catalytic CO_2 conversion; meanwhile, the CO_2 adsorption capability is also proposed to affect the CO_2 conversion efficiency, both of which could be valuable to exploit these new MOFs for future CO_2 capture and utilization.

Experimental Section

Preparation of Al(Sbpdc)(OH) (USTC-253), Al(bpdc)(OH) (EL-MIL-53), and Al(bpydc)(OH) (MOF-253)

A mixture of $Al(NO_3)_3{\cdot}9H_2O$ (260 mg, 0.69 mmol), organic linker (Sbpdc, 163 mg, 0.53 mmol; bpdc, 130 mg, 0.53 mmol; bpydc, 131 mg, 0.53 mmol), and DMF (15 mL) was sealed in a 20 mL Teflon-capped autoclave and heated at 393 K for two days. After cooling to RT, the resulting white products were washed with DMF three times then extracted with methanol for 24 h. Upon removal of the solvent and drying in vacuum at 80 °C, USTC-253, EL-MIL-53, and MOF-253 were obtained, respectively.

Preparation of USTC-253-TFA

A mixture of $Al(NO_3)_3{\cdot}9H_2O$ (260 mg, 0.69 mmol), Sbpdc (163 mg, 0.53 mmol), TFA (0.5 mL), and DMF (15 mL) was sealed in a Teflon-capped autoclave and heated at 393 K for two days. After cooling to RT, the resulting white product was washed with DMF three times then extracted with methanol for 24 h. Upon removal of the solvent and drying in vacuum at 80 °C, USTC-253-TFA was obtained.

Catalytic cycloaddition of CO_2 with epoxides

A mixture of propylene oxide (28.6 mmol), catalyst (0.289 mmol), and TBAB (1.86 mmol) was sealed in a 5 mL flask, which was connected to a balloon that contained 1 bar CO_2. The flask was kept at 298 K for 72 h.

Acknowledgements

This work is supported by the National Key Basic Research Program of China (2014CB931803), the NSFC (21371162 and 51301159), the Research Fund for the Doctoral Program of Higher Education of China (20133402120020), the Recruitment Program of Global Youth Experts, the Scientific Research Foundation for the Returned Overseas Chinese Scholars, the State Education Ministry, and the Fundamental Research Funds for the Central Universities (WK2060190026).

Keywords: aluminum · CO_2 capture · cycloaddition · heterogeneous catalysis · metal–organic frameworks

[1] a) G. T. Rochelle, *Science* **2009**, *325*, 1652 – 1654; b) R. J. Notz, I. Tonnies, N. McCann, G. Scheffknecht, H. Hasse, *Chem. Eng. Technol.* **2011**, *34*, 163 – 172.

[2] a) P. G. Jessop, T. Ikariya, R. Noyori, *Nature* **1994**, *368*, 231 – 233; b) T. Sakakura, Y. Saito, M. Okano, J.-C. Choi, T. Sako, *J. Org. Chem.* **1998**, *63*, 7095 – 7096; c) F. Shi, Y. Deng, T. SiMa, J. Peng, Y. Gu, B. Qiao, *Angew. Chem. Int. Ed.* **2003**, *42*, 3257 – 3260; *Angew. Chem.* **2003**, *115*, 3379 – 3382; d) T. Sakakura, J.-C. Choi, H. Yasuda, *Chem. Rev.* **2007**, *107*, 2365 – 2387; e) T. Jiang, X. Ma, Y. Zhou, S. Liang, J. Zhang, B. Han, *Green Chem.* **2008**, *10*, 465 – 469.

[3] a) A.-A. G. Shaikh, S. Sivaram, *Chem. Rev.* **1996**, *96*, 951 – 976; b) H. S. Kim, J. J. Kim, B. G. Lee, O. S. Jung, H. G. Jang, S. O. Kang, *Angew. Chem. Int. Ed.* **2000**, *39*, 4096 – 4098; *Angew. Chem.* **2000**, *112*, 4262 – 4264.

[4] a) K. Yamaguchi, K. Ebitani, T. Yoshida, H. Yoshida, K. Kaneda, *J. Am. Chem. Soc.* **1999**, *121*, 4526 – 4527; b) R. L. Paddock, S. T. Nguyen, *J. Am. Chem. Soc.* **2001**, *123*, 11498 – 11499; c) L. N. He, H. Yasuda, T. Sakakura, *Green Chem.* **2003**, *5*, 92 – 94; d) X. B. Lu, B. Liang, Y. J. Zhang, Y. Z. Tian, Y. M. Wang, C. X. Bai, H. Wang, R. Zhang, *J. Am. Chem. Soc.* **2004**, *126*, 3732 – 3733; e) X. B. Lu, Y. J. Zhang, K. Jin, L. M. Luo, H. Wang, *J. Catal.* **2004**, *227*, 537 – 541; f) Y. M. Shen, W.-L. Duan, M. Shi, *Eur. J. Org. Chem.* **2004**, 3080 – 3089; g) H. Yasuda, L. N. He, T. Sakakura, C. Hu, *J. Catal.* **2005**, *233*, 119 – 122; h) Y. Du, F. Cai, D.-L. Kong, L.-N. He, *Green Chem.* **2005**, *7*, 518 – 523.

[5] a) F. Shi, Q. Zhang, Y. Ma, Y. He, Y. Deng, *J. Am. Chem. Soc.* **2005**, *127*, 4182 – 4183; b) Y. Xie, Z. Zhang, T. Jiang, J. He, B. Han, T. Wu, K. Ding, *Angew. Chem. Int. Ed.* **2007**, *46*, 7255 – 7258; *Angew. Chem.* **2007**, *119*, 7393 – 7396; c) K. Motokura, S. Itagaki, Y. Iwasawa, A. Miyaji, T. Baba, *Green Chem.* **2009**, *11*, 1876 – 1880; d) E. A. Prasetyanto, M. B. Ansari, B.-H. Min, S.-E. Park, *Catal. Today* **2010**, *158*, 252 – 257; e) P. Ratnasamy, D. Srinivas, *Handbook of Heterogeneous Catalysis, 2nd ed.*; Wiley-VCH: New York, 2008; f) R. Srivastava, T. H. Bennur, D. Srinivas, *J. Mol. Catal. A* **2005**, *226*, 199 – 205.

[6] a) S. Horike, S. Shimomura, S. Kitagawa, *Nat. Chem.* **2009**, *1*, 695 – 704; b) J. R. Long, O. M. Yaghi, *Chem. Soc. Rev.* **2009**, *38*, 1213 – 1214; c) H.-C. Zhou, J. R. Long, O. M. Yaghi, *Chem. Rev.* **2012**, *112*, 673 – 674; d) H.-C. Zhou, S. Kitagawa, *Chem. Soc. Rev.* **2014**, *43*, 5415 – 5418; e) H. Furukawa, K. E. Cordova, M. O'Keeffe, O. M. Yaghi, *Science* **2013**, *341*, 6149.

[7] a) K. Sumida, D. L. Rogow, J. A. Mason, T. M. McDonald, E. D. Bloch, Z. R. Herm, T.-H. Bae, J. R. Long, *Chem. Rev.* **2012**, *112*, 724 – 781; b) M. P. Suh, H. J. Park, T. K. Prasad, D.-W. Lim, *Chem. Rev.* **2012**, *112*, 782 – 835; c) J.-R. Li, J. Sculley, H.-C. Zhou, *Chem. Rev.* **2012**, *112*, 869 – 932; d) Y. He, W. Zhou, G. Qian, B. Chen, *Chem. Soc. Rev.* **2014**, *43*, 5657 – 5678; e) X. Zhao, D. Sun, S. Yuan, S. Feng, R. Cao, D. Yuan, S. Wang, J. Dou, D. Sun, *Inorg. Chem.* **2012**, *51*, 10350 – 10355; f) Y.-P. He, Y.-X. Tan, J. Zhang, *Chem. Commun.* **2013**, *49*, 11323 – 11325; g) J.-S. Qin, D.-Y. Du, W.-L. Li, J.-P. Zhang, S.-L. Li, Z.-M. Su, X.-L. Wang, Q. Xu, K.-Z. Shao, Y.-Q. Lan, *Chem. Sci.* **2012**, *3*, 2114 – 2118; h) C. A. Fernandez, J. Liu, P. K. Thallapally, D. M. Strachan, *J. Am. Chem. Soc.* **2012**, *134*, 9046 – 9049.

[8] a) B. Chen, S. Xiang, G. Qian, *Acc. Chem. Res.* **2010**, *43*, 1115 – 1124; b) H.-L. Jiang, Y. Tatsu, Z.-H. Lu, Q. Xu, *J. Am. Chem. Soc.* **2010**, *132*, 5586 – 5587; c) Y. Takashima, V. Martinez, S. Furukawa, M. Kondo, S. Shimomura, H. Uehara, M. Nakahama, K. Sugimoto, S. Kitagawa, *Nat. Commun.* **2011**, *2*, 168 (1-8); d) L. E. Kreno, K. Leong, O. K. Farha, M. Allendorf, R. P. Van

Duyne, J. T. Hupp, *Chem. Rev.* **2012**, *112*, 1105 – 1125; e) J.-W. Zhang, H.-T. Zhang, Z.-Y. Du, X. Wang, S.-H. Yu, H.-L. Jiang, *Chem. Commun.* **2014**, *50*, 1092 – 1094; f) R.-B. Lin, F. Li, S.-Y. Liu, X.-L. Qi, J.-P. Zhang, X.-M. Chen, *Angew. Chem. Int. Ed.* **2013**, *52*, 13429 – 13433; *Angew. Chem.* **2013**, *125*, 13671 – 13675; g) Z. Hu, B. J. Deibert, J. Li, *Chem. Soc. Rev.* **2014**, *43*, 5815 – 5817; h) M. Zhang, G. Feng, Z. Song, Y.-P. Zhou, H.-Y. Chao, D. Yuan, T. T. Y. Tan, Z. Guo, Z. Hu, B. Z. Tang, B. Liu, D. Zhao, *J. Am. Chem. Soc.* **2014**, *136*, 7241 – 7244.

[9] a) Z. Wang, S. M. Cohen, *Chem. Soc. Rev.* **2009**, *38*, 1315 – 1329; b) S. C. Sahoo, T. Kundu, R. Banerjee, *J. Am. Chem. Soc.* **2011**, *133*, 17950 – 17958; c) J. An, S. J. Geib, N. L. Rosi, *J. Am. Chem. Soc.* **2009**, *131*, 8376 – 8377; d) P. Horcajada, R. Gref, T. Baati, P. K. Allan, G. Maurin, P. Couvreur, G. Férey, R. E. Morris, C. Serre, *Chem. Rev.* **2012**, *112*, 1232 – 1268; e) P. Ramaswamy, N. E. Wong, G. K. H. Shimizu, *Chem. Soc. Rev.* **2014**, *43*, 5913 – 5916; f) T. K. Kim, K. J. Lee, J. Y. Cheon, J. H. Lee, S. H. Joo, H. R. Moon, *J. Am. Chem. Soc.* **2013**, *135*, 8940 – 8946.

[10] S. R. Caskey, A. G. Wong-Foy, A. J. Matzger, *J. Am. Chem. Soc.* **2008**, *130*, 10870 – 10871.

[11] a) J. S. Seo, D. Whang, H. Lee, S. I. Jun, J. Oh, Y. J. Jeon, K. Kim, *Nature* **2000**, *404*, 982 – 986; b) L. Ma, C. Abney, W. Lin, *Chem. Soc. Rev.* **2009**, *38*, 1248 – 1256; c) D. Farrusseng, S. Aguado, C. Pinel, *Angew. Chem. Int. Ed.* **2009**, *48*, 7502 – 7513; *Angew. Chem.* **2009**, *121*, 7638 – 7649; d) A. Corma, H. García, F. X. L. I. Xamena, *Chem. Rev.* **2010**, *110*, 4606 – 4655; e) H.-L. Jiang, Q. Xu, *Chem. Commun.* **2011**, *47*, 3351 – 3370; f) Y. Fu, D. Sun, Y. Chen, R. Huang, Z. Ding, X. Fu, Z. Li, *Angew. Chem. Int. Ed.* **2012**, *51*, 3364 – 3367; *Angew. Chem.* **2012**, *124*, 3420 – 3423; g) J. Gascon, A. Corma, F. Kapteijn, F. X. L. I. Xamena, *ACS Catal.* **2014**, *4*, 361 – 378; h) J. Liu, L. Chen, H. Cui, J. Zhang, L. Zhang, C.-Y. Su, *Chem. Soc. Rev.* **2014**, *43*, 6011 – 6012.

[12] a) J. Liu, P. K. Thallapally, B. P. McGrail, D. R. Brown, J. Liu, *Chem. Soc. Rev.* **2012**, *41*, 2308 – 2322; b) H.-L. Jiang, D. Feng, T.-F. Liu, J.-R. Li, H.-C. Zhou, *J. Am. Chem. Soc.* **2012**, *134*, 14690 – 14693; c) F. Luo, M.-S. Wang, M.-B. Luo, G.-M. Sun, Y.-M. Song, P.-X. Li, G.-C. Guo, *Chem. Commun.* **2012**, *48*, 5989 – 5991; d) Y. Hu, W. M. Verdegaal, S.-H. Yu, H.-L. Jiang, *ChemSusChem* **2014**, *7*, 734 – 737.

[13] a) H. Wu, Y. S. Chua, V. Krungleviciute, M. Tyagi, P. Chen, T. Yildirim, W. Zhou, *J. Am. Chem. Soc.* **2013**, *135*, 10525 – 10532; b) F. Vermoortele, B. Bueken, G. L. Bars, B. Van de Voorde, M. Vandichel, K. Houthoofd, A. Vimont, M. Daturi, M. Waroquier, V. Van Speybroeck, C. Kirschhock, D. E. De Vos, *J. Am. Chem. Soc.* **2013**, *135*, 11465 – 11468; c) O. Kozachuk, I. Luz, F. X. L. I. Xamena, H. Noei, M. Kauer, H. B. Albada, E. D. Bloch, B. Marler, Y. Wang, M. Muhler, R. A. Fischer, *Angew. Chem. Int. Ed.* **2014**, *53*, 7058 – 7062; *Angew. Chem.* **2014**, *126*, 7178 – 7182; d) Z. Zhang, Y. Zhao, Q. Gong, Z. Li, J. Li, *Chem. Commun.* **2013**, *49*, 653 – 661.

[14] a) J. Song, Z. Zhang, S. Hu, T. Wu, T. Jiang, B. Han, *Green Chem.* **2009**, *11*, 1031 – 1036; b) E. E. Maciasa, P. Ratnasamy, M. A. Carreon, *Catal. Today* **2012**, *198*, 215 – 218; c) C. M. Miralda, E. E. Macias, M. Zhu, P. Ratnasamy, M. A. Carreon, *ACS Catal.* **2012**, *2*, 180 – 183; d) J. Kim, S.-N. Kim, H.-G. Jang, G. Seo, W.-S. Ahn, *Appl. Catal. A* **2013**, *453*, 175 – 180; e) M. Zhu, D. Srinivas, S. Bhogeswararao, P. Ratnasamy, M. A. Carreon, *Catal. Commun.* **2013**, *32*, 36 – 40; f) D.-A. Yang, H.-Y. Cho, J. Kim, S.-T. Yang, W.-S. Ahn, *Energy Environ. Sci.* **2012**, *5*, 6465 – 6473; g) D. Feng, W.-C. Chung, Z. Wei, Z.-Y. Gu, H.-L. Jiang, Y.-P. Chen, D. J. Darensbourg, H.-C. Zhou, *J. Am. Chem. Soc.* **2013**, *135*, 17105 – 17110.

[15] a) W.-Y. Gao, Y. Chen, Y. Niu, K. Williams, L. Cash, P. J. Perez, L. Wojtas, J. Cai, Y.-S. Chen, S. Ma, *Angew. Chem. Int. Ed.* **2014**, *53*, 2615 – 2619; *Angew. Chem.* **2014**, *126*, 2653 – 2657; b) W.-Y. Gao, L. Wojtas, S. Ma, *Chem. Commun.* **2014**, *50*, 5316 – 5318.

[16] a) I. Senkovska, F. Hoffmann, M. Fröba, J. Getzschmann, W. Böhlmann, S. Kaskel, *Microporous Mesoporous Mater.* **2009**, *122*, 93 – 98; b) E. D. Bloch, D. Britt, C. Lee, C. J. Doonan, F. J. Uribe-Romo, H. Furukawa, J. R. Long, O. M. Yaghi, *J. Am. Chem. Soc.* **2010**, *132*, 14382 – 14384.

[17] A. Schaate, P. Roy, A. Godt, J. Lippke, F. Waltz, M. Wiebcke, P. Behrens, *Chem. Eur. J.* **2011**, *17*, 6643 – 6651.

[18] P. Xydias, I. Spanopoulos, E. Klontzas, G. E. Froudakis, P. N. Trikalitis, *Inorg. Chem.* **2014**, *53*, 679 – 681.

[19] a) R.-Q. Zou, H. Sakurai, S. Han, R.-Q. Zhong, Q. Xu, *J. Am. Chem. Soc.* **2007**, *129*, 8402 – 8403; b) U. Ravon, G. Chaplais, C. Chizallet, B. Seyyedi, F. Bonino, S. Bordiga, N. Bats, D. Farrusseng, *ChemCatChem* **2010**, *2*, 1235 – 1238.

[20] T. Ben, Y. Li, L. Zhu, D. Zhang, D. Cao, Z. Xiang, X. Yao, S. Qiu, *Energy Environ. Sci.* **2012**, *5*, 8370 – 8376.

[21] a) K. S. Park, Z. Ni, A. P. Cote, J. Y. Choi, R. D. Huang, F. J. Uribe-Romo, H. K. Chae, M. O'Keeffe, O. M. Yaghi, *Proc. Natl. Acad. Sci. USA* **2006**, *103*, 10186 – 10191; b) X. C. Huang, Y. Y. Lin, J. P. Zhang, X. M. Chen, *Angew. Chem. Int. Ed.* **2006**, *45*, 1557 – 1559; *Angew. Chem.* **2006**, *118*, 1587 – 1589; c) G. Férey, C. Mellot-Draznieks, C. Serre, F. Millange, J. Dutour, S. Surblé, I. Margiolaki, *Science* **2005**, *309*, 2040 – 2042; d) J. H. Cavka, S. Jakobsen, U. Olsbye, N. Guillou, C. Lamberti, S. Bordiga, K. P. Lillerud, *J. Am. Chem. Soc.* **2008**, *130*, 13850 – 13851; e) T. Loiseau, C. Serre, C. Huguenard, G. Fink, F. Taulelle, M. Henry, T. Bataille, G. Férey, *Chem. Eur. J.* **2004**, *10*, 1373 – 1382.

Received: November 5, 2014
Revised: December 1, 2014
Published online on February 4, 2015